



# A novel coplanar waveguide resonator on flexible substrate



Yu Ming Wei<sup>a</sup>, Xu Guang Guo<sup>b,\*</sup>, Lin Chen<sup>a,\*</sup>, Yi Ming Zhu<sup>a</sup>

<sup>a</sup> Shanghai Key Lab of Modern Optical System and Engineering Research Center of Optical Instrument and System, Ministry of Education, University of Shanghai for Science and Technology, Shanghai 200093, China

<sup>b</sup> Key Laboratory of Terahertz Solid-State Technology, Shanghai Institute of Microsystem and Information Technology, Chinese Academy of Sciences, 865 Changning Road, Shanghai 200050, China

## ARTICLE INFO

### Article history:

Received 2 June 2016

Accepted 30 July 2016

### Keywords:

Coplanar waveguide

Split ring resonators

Flexible substrate

Millimeter wave chip

## ABSTRACT

In this paper a flexible coplanar waveguide resonator with high quality factor is proposed and fabricated. The device consists of a compact coplanar waveguide (CPW) and two complementary split rectangle resonators (CSRR) locating between the central signal wire and the ground plane of the CPW. The designed and measured values of frequency, attenuation, and quality factor of the resonant dips are 31.9 GHz and 31.8 GHz, −45 dB and −12 dB, and 115.7 and 35.1, respectively. The differences between the simulated and measured values of attenuation and quality factor are due to the imperfect metal structure. The frequency of the resonant dip is very sensitive to dielectric environment. This chip device is very promising for biomedical and sensing applications.

© 2016 Elsevier GmbH. All rights reserved.

## 1. Introduction

The development of terahertz technology is very fast in recent years. Terahertz functional devices play the important roles in many applications [1–5]. Among them, the sensing devices based on the coplanar waveguides (CPWs) have received growing interests [5]. CPW offers a variety of advantages over the conventional microstrip lines, such as the easy facilitation of shunts as well as the series surface mounting of active and passive devices and the reduction of fabrication costs [5]. Because of their convenient fabrication and integration, CPWs have been widely applied in integrated circuits, trace amounts of biological and chemical analysis, micro fluidic detection, etc. [6,7].

In order to apply the CPWs to microwave and terahertz circuit with high quality factor, the fabrication processes must be compatible with planar circuit technology. In the previous work, the CPW loaded with planar metamaterial resonators have been constructed by placing split ring resonators (SRRs) in the gap of the CPW [8]. Due to the magnetic resonance, there exists a band stop in the transmission spectrum for such CPW-SRR structures. However, the structural impedances of the CPW and the SRRs are mismatch, resulting in a large return loss. To overcome the mismatch problem, the SRRs are placed on the bottom side of the dielectric layer. This structure limits its application because of complicated fabrication of multilayer structure [9,10]. To resolve these problems, complementary split ring resonator or complementary split rectangle resonator are integrated into CPW, owing to their better performance [11,12]. In addition, in the single layer plane technology, resonator elements can be either integrated in the “inner” or “outer” conductor of the CPW. A series of CPW planar resonators have already been proposed [13,14].

\* Corresponding authors.

E-mail addresses: [xgguo@mail.sim.ac.cn](mailto:xgguo@mail.sim.ac.cn) (X.G. Guo), [linchen@usst.edu.cn](mailto:linchen@usst.edu.cn) (L. Chen).

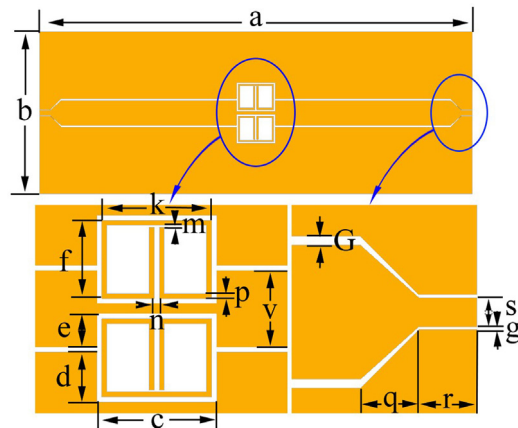


**Fig. 1.** The top view of the device. The length and the width of our CPW-CSRR device are  $a = 8$  mm and  $b = 3$  mm. The center conductor  $s$  and slot width  $g$  at the input and output ports are all  $100\ \mu\text{m}$  and  $10\ \mu\text{m}$ . The center conductor  $v$  and slot width  $G$  in the middle of the CPW are  $460\ \mu\text{m}$  and  $30\ \mu\text{m}$ . The tapers have the separation of  $n = 30\ \mu\text{m}$ , the width of  $p = 30\ \mu\text{m}$ , and the slit of  $m = 10\ \mu\text{m}$ . The length and width of the resonator are  $k = 660\ \mu\text{m}$  and  $f = 470\ \mu\text{m}$ . The other parameters of the CSRR are  $e = 200\ \mu\text{m}$ ,  $d = 300\ \mu\text{m}$  and  $c = 720\ \mu\text{m}$ , respectively.

In this paper we present a device which is fully compatible with a lab-on-chip approach. We integrate the resonant structure into a CPW, which is metalized only in one layer and, hence, is more compact than the structure reported in [9,10]. The CPW-CSRR structure is fabricated on a  $125\ \mu\text{m}$  thick polyethylene naphthalate (PEN) flexible substrate which can bend the transmission direction in a large angle range. Such arbitrary bending transfer characteristics bring convenience for constructing the compact sensing and detection systems in microwave and terahertz regimes.

## 2. Structure design and fabrication

Our CPW-CSRR chip structure was fabricated with  $0.5\ \mu\text{m}$  thick gold film on a  $125\ \mu\text{m}$  thick flexible PEN film substrate by conventional photolithography [15–18]. The PEN film is thin enough to offer high flexibility for applications on non-planar surfaces. The resonators are symmetrically etched on the top layer. The top view of our device and the geometric parameters of the unit cell are depicted in Fig. 1. The length and the width of our CPW-CSRR device are  $a = 8$  mm and  $b = 3$  mm. The center conductor  $s$  and slot width  $g$  at the input and output ports are all  $100\ \mu\text{m}$  and  $10\ \mu\text{m}$ , which are chosen to obtain a characteristic impedance matching with the probe impedance of  $Z_0 = 50\ \Omega$ . The center conductor  $v$  and slot width  $G$  in the middle of the CPW are  $460\ \mu\text{m}$  and  $30\ \mu\text{m}$ . We added two CPW tapers to connect the input and output ports to the main body of the CPW-CSRR structure. Such CPW tapers can effectively reduce the return loss. The tapers have the separation of  $n = 30\ \mu\text{m}$ , the width of  $p = 30\ \mu\text{m}$ , and the slit of  $m = 10\ \mu\text{m}$ . The length and width of the resonator are  $k = 660\ \mu\text{m}$  and  $f = 470\ \mu\text{m}$ . The other parameters of the CSRR are  $e = 200\ \mu\text{m}$ ,  $d = 300\ \mu\text{m}$  and  $c = 720\ \mu\text{m}$ , respectively. Our simulation is performed with the computer simulation technology (CST) Microwave Studio with frequency domain solver using perfect boundary conditions [19]. The parameters were optimized through simulation to obtain the maximum values of quality factor and intensity of local electromagnetic field. The PEN substrate with relative permittivity  $\epsilon_{pi} = 2.56$  is modeled as a lossy dielectric medium with a loss tangent of 0.003 and gold is simulated with a conductivity of  $\sigma_{AU} = 4.561 \times 10^7\ \text{S/m}$  (behave almost like perfect conductor compared to visible region [20]).

Fig. 2(a) and (b) show the optical microscope images of the resonant structure and the photograph of the final flexible thin sample. We use the standard lift-off process to get the sample which is fully compatible with a lab-on-chip approach. The S-parameters of the fabricated CPW-CSRR sample are measured with a probe station equipped with two  $150\text{-}\mu\text{m}$ -pitch ground-signal-ground (GSG) microprobes connected to an N5245A vector network analyzer (VNA) within the frequency range of 1–39 GHz. Calibration of the CPW-CSRR with open circuit, short circuit, load and direct connection are performed.

## 3. Results and analysis

The simulated and measured insertion losses are shown in Fig. 3a and b. The simulated and measured transmission resonance dips are centered at 31.9 GHz and 31.8 GHz, respectively, which are well consistent with each other. The simulated insertion loss is lower than  $-45\ \text{dB}$  for the resonant dip, and the corresponding quality factor is about 115.7. However, the measured results of the CPW-CSRR sample do not show such strong resonant behavior. The measured insertion loss of the resonant dip is lower than  $-12\ \text{dB}$  and the quality factor is about 35.1. Differences between experimental and simulated results may be attributed to the error of fabrication, such as the slight unequal gap between the signal line and the ground wire, the Ohmic loss duo to the smoothless surface, the roughness of the edges, the sharp metal corner, and the defects in the metal-dielectrics interface. All these factors cannot be considered quantitatively in our simulations.

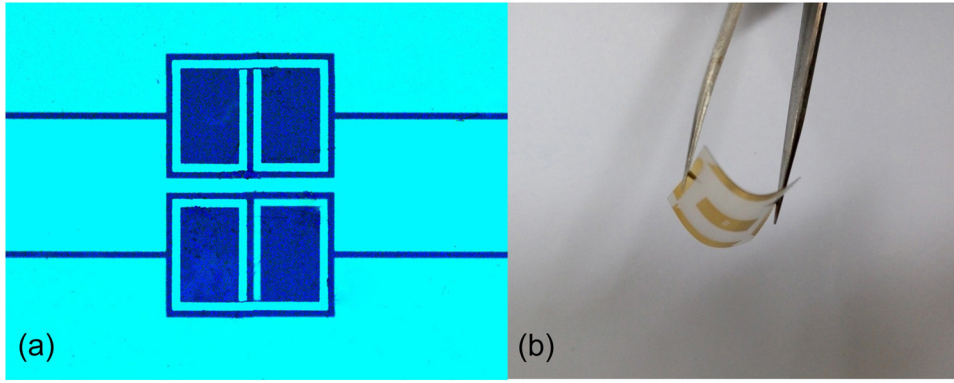


**Fig. 2.** (a) The optical microscope images of the resonant structure. (b) The photograph of the final flexible thin sample.

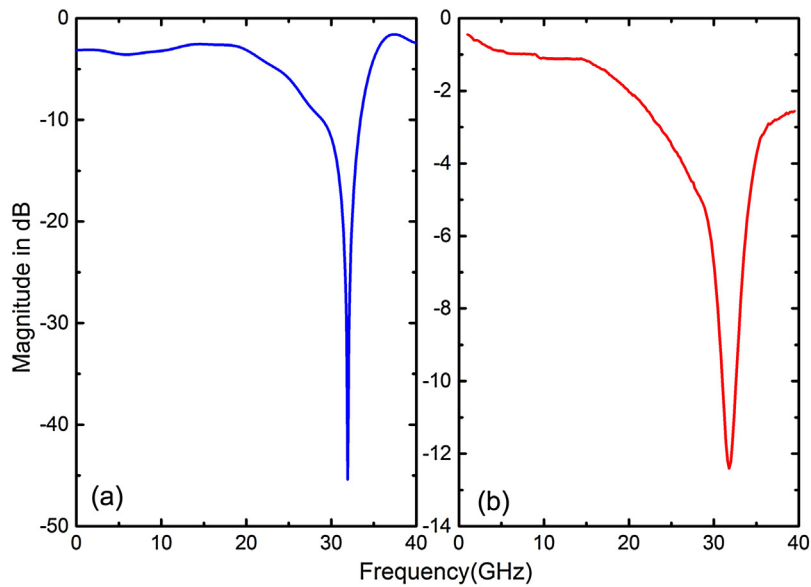


**Fig. 3.** (a) Simulated and (b) experimental transmission spectra of CPW measured by using the VNA.

Here, we discuss the origin of this sharp resonant dip at 31.9 GHz. In the low frequency transmission region, the CPW has a fixed transmission mode [21–24]. The resonators in the middle of the device interfere with the electric field and the magnetic field of the transmission line. This interference changes the effective capacitance and inductance of the CPW line, which generates the transmission resonance dip. At the resonant frequency, the electric field intensity on the chip is several times larger than that of the free space. As shown in Fig. 4(a), the electric field is mainly concentrated in the middle of the resonators between two rods. The electric field distribution in Fig. 4(b) is the cause of the transmission resonance dip. And Fig. 4(c) is the electric field distribution of the energy that has not been cut off. The electric field energy (31.9 GHz) is mainly localized in the 365  $\mu\text{m}$  scope above the CPW-CSRR structure in the vertical direction. For sensing application, the designed CPW-CSRR structure not only increases the interaction section between the sensor chip and the sample, but also greatly enhances the difference between the sample parameters (such as dielectric coefficient, absorption coefficient). Therefore, the detection accuracy is greatly improved.

In addition, we study the effect of the gap  $m$  on the quality factor of the whole structure. The simulation results in Fig. 5 show the different resonant frequencies and insertion losses corresponding to different  $m$  values. On the whole, the insertion loss decreases with the increase of the value of  $m$ . The transmission dip frequency shows a tendency to increase with increasing the value of  $m$ , a clear blue shift of the transmission dip can be observed. As the gap  $m$  increases the effective capacitance decreases and hence the transmission dip shift to higher frequencies. We can easily adjust the transmission dip frequency according to different requirements.

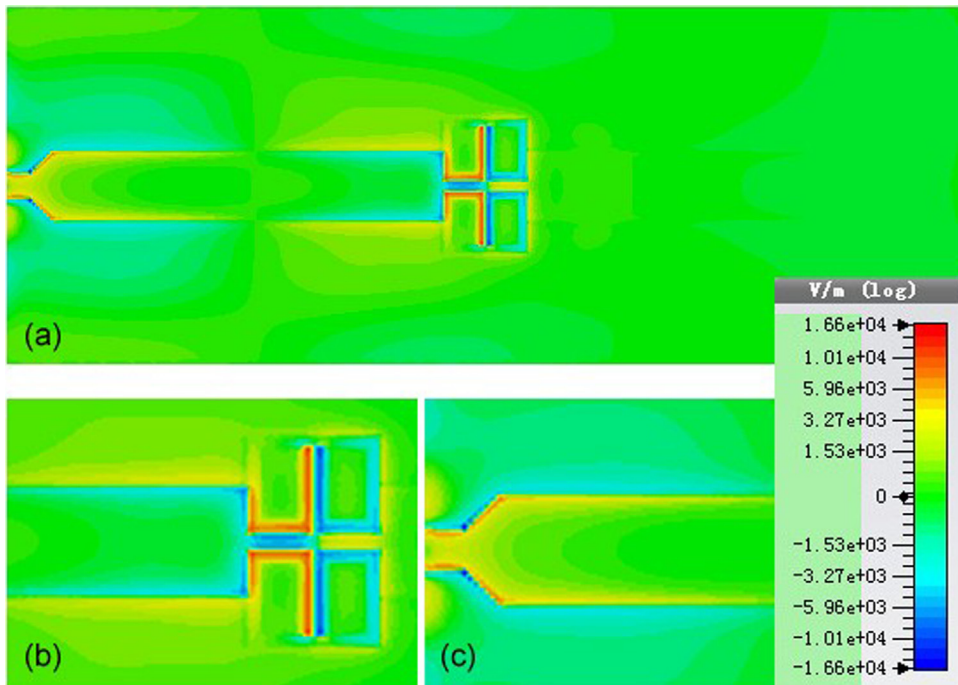


**Fig. 4.** (a) The electric field distributions of the CPW-CSRR at low-frequency resonance dip 31.9 GHz; (b) the electric field distribution of resonators; (c) the electric field distribution of the energy that has not been cut off.

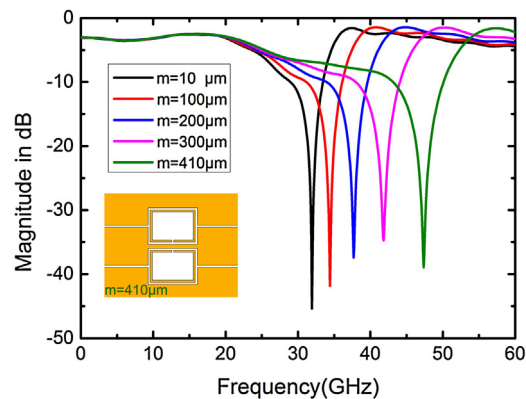


**Fig. 5.** The different insertion losses corresponding to different  $m$  values.

#### 4. Summary

In conclusion, we have proposed and demonstrated a novel CPW resonator on a flexible PEN substrate. The CPW chip presented meets the requirements of easy integration and compatibility with standard planar fabrication technique. The simulated transmission resonance dip is centered at 31.9 GHz with insertion loss of lower than  $-45$  dB and the quality factor of about 115.7. The measured transmission resonance dip is centered at 31.8 GHz with insertion loss of lower than  $-12$  dB and quality factor of about 35.1. The optimized design of the structure makes the electric field focus on the two rods in the resonators. It is very promising for biomedical and sensing applications, because it not only increases the interaction section, but also increases the sensitivity.

#### Acknowledgments

This work was partly supported by the National Program on Key Basic Research Project of China (973 Program, 2014CB339806), Basic Research Key Project (12JC1407100), Major National Development Project of Scientific Instrument and Equipment (2011YQ150021) (2012YQ14000504), National Natural Science Foundation of China (11174207)

(61138001) (61205094) (61307126), Shanghai Rising-Star Program(14QA1403100), Program of Shanghai Subject Chief Scientist (14XD1403000), Hujiang Foundation of China (C14002), Zhejiang Key Discipline of Instrument Science and Technology (JL150505), and the New Century Excellent Talents Project from the Ministry of Education (NCET-12-1052).

## References

- [1] L. Chen, Y. Zhu, X. Zang, B. Cai, Z. Li, L. Xie, S.L. Zhuang, Mode splitting transmission effect of surface wave excitation through a metal hole array, *Light Sci. Appl.* 2 (3) (2013) e60.
- [2] L. Chen, C. Gao, J. Xu, X.F. Zang, B. Cai, Y.M. Zhu, Observation of electromagnetically induced transparency-like transmission in terahertz asymmetric waveguide-cavities systems, *Opt. Lett.* 38 (9) (2013) 1379–1381.
- [3] L. Chen, J. Xu, C. Gao, X.F. Zang, B. Cai, Y.M. Zhu, Manipulating terahertz electromagnetic induced transparency through parallel plate waveguide cavities, *Appl. Phys. Lett.* 103 (25) (2013) 251105.
- [4] L. Chen, Z. Cheng, J. Xu, X. Zang, B. Cai, Y. Zhu, Controllable multiband terahertz notch filter based on a parallel plate waveguide with a single deep groove, *Opt. Lett.* 39 (15) (2014) 4541–4544.
- [5] A.M. Watson, A. Padilla, C.L. Holloway, et al., High-Q on-chip microwave resonator for sensitive permittivity detection in nanoliter volumes, *Solid-State Sensors, Actuators and Microsystems (TRANSDUCERS) Transducers-2015 18th International Conference on IEEE* (2015) 1665–1668.
- [6] T. Chretiennot, D. Dubuc, K. Grenier, A microwave and microfluidic planar resonator for efficient and accurate complex permittivity characterization of aqueous solutions, *IEEE Trans. Microw. Theory Tech.* 61 (2) (2013) 972–978.
- [7] N. Meyne, S. Latus, A.F. Jacob, Corrugated coplanar transmission-Line sensor for broadband liquid sample characterization, in: *Microwave Conference (GeMIC), 2014 German, VDE, 2014*, pp. 1–4.
- [8] F. Falcone, F. Martin, J. Bonache, et al., Coplanar waveguide structures loaded with split-ring resonators, *Microw. Opt. Technol. Lett.* 40 (1) (2004) 3–6.
- [9] A.K. Panda, K.S. Sahu, R.K. Mishra, A compact triangular SRR loaded CPW line and its use in highly selective wideband bandpass filter for WiMAX communication system, *Computers and Devices for Communication (CODEC), 2012 5th International Conference On. IEEE* (2012) 1–4.
- [10] F. Martín, F. Falcone, J. Bonache, et al., Miniaturized coplanar waveguide stop band filters based on multiple tuned split ring resonators, *IEEE Microw. Wirel. Compon. Lett.* 13 (12) (2003) 511–513.
- [11] I.A. Ibraheem, M. Koch, Coplanar waveguide metamaterials: the role of bandwidth modifying slots, *Appl. Phys. Lett.* 91 (11) (2007) 113517.
- [12] I.A.I. Al-Naib, M. Koch, Higher degree of miniaturization with split rectangle resonators, *Microwave Conference, 2008. EuMC 2008. 38th European. IEEE* (2008) 559–562.
- [13] L.P. Katehi, Miniature stub and filter designs using the microshield transmission line, *Microw. Symp. Dig.* 2 (1995) 675–678.
- [14] K. Hettak, N. Dib, A.F. Sheta, et al., A class of novel uniplanar series resonators and their implementation in original applications, *IEEE Trans. Microw. Theory Tech.* 46 (9) (1998) 1270–1276.
- [15] Z. Cheng, L. Chen, X. Zang, B. Cai, Y. Peng, Y.M. Zhu, Ultrathin dual-mode filtering characteristics of terahertz metamaterials with electrically unconnected and connected U-shaped resonators array, *Opt. Commun.* 342 (2015) 20–25.
- [16] Y. Shan, L. Chen, C. Shi, Z.X. Cheng, X.F. Zang, B.Q. Xu, Y.M. Zhu, Ultrathin flexible dual band terahertz absorber, *Opt. Commun.* 350 (2015) 63–70.
- [17] L. Chen, Y.M. Wei, X.F. Zang, Y.M. Zhu, S.L. Zhuang, Excitation of dark multipolar plasmonic resonances at terahertz frequencies, *Sci. Rep.* 6 (2016) 22027.
- [18] Z. Cheng, L. Chen, X. Zang, B. Cai, Y. Peng, Y.M. Zhu, Tunable plasmon-induced transparency effect based on self-asymmetric H-shaped resonators meta-atoms, *J. Opt.* 17 (3) (2015) 035103.
- [19] CST Microwave Studio®, <http://www.cst.com/Content/Products/MWS/Overview.aspx>.
- [20] L. Chen, Z.Q. Cao, F. Ou, H.G. Li, Q.S. Shen, H.C. Qiao, Observation of large positive and negative lateral shifts of a reflected beam from symmetrical metal-cladding waveguides, *Opt. Lett.* 32 (2007) 1432–1434.
- [21] R.N. Simons, R.K. Arora, Coupled slot line field components, *IEEE Trans. Microw. Theory Tech.* 7 (30) (1982) 1094–1099.
- [22] R. Garg, I. Bahl, M. Bozzi, *Microstrip Lines and Slotlines*, Artech house, 2013.
- [23] R.N. Simons, *Coplanar Waveguide Circuits, Components, and Systems*, John Wiley & Sons, 2004.
- [24] L. Cao, A.S. Grimault-Jacquín, N. Zerounian, et al., Design and VNA-measurement of coplanar waveguide (CPW) on benzocyclobutene (BCB) at THz frequencies, *Infrared Phys. Technol.* 63 (2014) 157–164.